Influence of pump bandwidth and wavelength-drift on laser performance of solid-state Tm laser

Wang Juan[1,2], Huang Haizhou[1,2], Huang Jianhong[1], Ge Yan[1], Dai Shutao[1,2], Deng Jing[1], Lin Zixiong[1], Weng Wen[1], Lin Wenxiong[1]

(1. Key Laboratory of Optoelectronic Materials Chemistry and Physics, Fujian Institute of Research on the Structure of Matter, Chinese Academy of Sciences, Fuzhou 350002, China; 2. University of Chinese Academy of Sciences, Beijing 100049, China)

Abstract: In order to study the influence of pump bandwidth and wavelength-drift on the performance of solid-state lasers, theoretical analyses were performed on a quasi-three-level Tm:YAG laser, and the corresponding theoretical models, including both spectral and thermal models, were presented. In the Tm laser experiment, a compact and high-efficiency composite Tm laser operating at 2 013.2 nm was demonstrated, which was end-pumped by volume Bragg gratings (VBGs) locked laser diode (LD) with emission wavelength centered at 784.9 nm and bandwidth as narrow as 0.1 nm (full width at the half maximum, FWHM). A maximum output power of 7.96 W was obtained with a slope efficiency of 62.5% and optical conversion efficiency of 53.3%, respectively. The maximum laser wavelength drifted from 2 013.25 nm to 2 014.53 nm when increasing the absorbed pump power from 1.87 W to 14.93 W for the 3% output coupling. As for 5% output coupling, the drift was from 2 013.91 nm to 2 014.26 nm. It was found that a narrow LD bandwidth of 0.1 nm resulted in a more pronounced excitation efficiency and thus a higher laser efficiency, despite that the maximum temperature within the crystal was slightly higher. The present study could be extended to other solid-state lasers for the choice of pump source by comprehensively considering the pump bandwidth and wavelength-drift and the spectral profiles of gain medium, which would be helpful for an efficient laser system.

Key words: pump bandwidth; wavelength-drift; thermal effect; 2 μm laser; excitation efficiency

CLC number: TN248.1 **Document code:** A **DOI:** 10.3788/IRLA201948.0405002

泵浦线宽和波长飘移对全固态 Tm 激光器性能的影响

王 娟[1,2],黄海洲[1,2],黄见洪[1],葛 燕[1],戴殊韬[1,2],邓 晶[1],林紫雄[1],翁 文[1],林文雄[1]

(1. 中国科学院福建物质结构研究所 光电材料化学和物理重点实验室,福建 福州 350002;
2. 中国科学院大学,北京 100049)

摘 要: 为了研究泵浦带宽和波长飘移对全固态激光器的影响,进行了光谱分析和热效应分析,该分析是在准三能级 Tm:YAG 激光器上进行的。提出光谱模型和晶体热模型,用来研究不同泵浦带宽下

收稿日期: 2018-11-26; **修订日期:** 2018-12-17

基金项目: 国家重点研发计划(2017YFB1104502,2016YFB0701004)

作者简介: 王娟(1990-),女,硕士生,主要从事中红外激光器和 3D 打印方面的研究。Email:wangjuan@fjirsm.ac.cn

导师简介: 林文雄(1966-),男,研究员,博士生导师,博士,主要从事激光器、非线性光学材料和 3D 打印方面的研究。Email:wxlin@fjirsm.ac.cn

Tm 激光器的效率和热效应。在 Tm 激光实验中,结构紧凑、高效率的键合 Tm 激光器得到验证,中心波长输出在 2 013.2 nm。这一激光器的泵浦源是 0.1 nm 窄线宽的光纤耦合激光二极管,其输出波长是 784.9 nm。最大输出功率为 7.96 W,斜率效率为 62.5%,光-光转换效率为 53.3%。当耦合透过率为 3% 时,激光功率从 1.87 W 增大到 14.93 W,激光波长从 2 013.25~2 014.53 nm 飘移。当耦合透过率为 5% 时,输出波长从 2 013.91 nm 飘移到 2 014.26 nm。尽管晶体的最高温度会稍有上升,但 0.1 nm 窄带宽泵浦可以有效提高激发效率,因此具有更高的激光效率。通过综合考虑泵浦带宽和波长飘移以及增益介质的光谱分布,该研究可以扩展到其他固体激光器来选择泵浦源,有助于实现高效的激光系统。

关键词:泵浦线宽; 波长飘移; 热效应; 2 μm 激光器; 激发效率

0 Introduction

Pump bandwidth and wavelength drift of pump source are important factors to be considered when designing an efficient solid-state laser. Former researchers have recognized the importance of pump spectral property by considering the spectral overlap between the measured absorption spectrum of gain medium and the emission profile of pump source[1-4]. Rare-earth doped bulk gain media usually exhibit narrow absorption peaks, i.e. the 3 -5 nm width resonant absorption peaks around 1.9 μm in Ho:YAG crystal[5]. Hence, when using an over 15 nm broad-band 1.9 μm LD pump source, which has significant wavelength-drift (1.3 nm/℃ [1]) with the cooling temperature or the driven current, an efficient absorption coefficient was considered for characterizing the laser efficiency of 1.9 μm LD pumped Ho laser[2]. In our recent work, such an efficient absorption was also taken into account in intra-cavity pumped Ho laser, where significant wavelength-drift in intra-cavity Tm laser around absorption side-band of Ho:YAG crystal was observed[3]. However, no further comprehensive research was carried out on the influence of pump spectral properties on both spectral efficiencies and thermal effects of the designed solid-state lasers.

Eye-safe 2 μm lasers from trivalent thulium ion (Tm^{3+}) is widely used in diverse fields such as remote sensing, laser ranging, and high-resolution spectroscopy[6-10]. 2 μm lasers can also be used as the pump source for realizing optical parametric oscillator (OPO) and optical parametric amplifier (OPA). Doped in host crystals, Tm^{3+} ion features a long upper level lifetime for laser radiation, and the characterized "2 for 1" cross-relaxation[11], thus capable to realize high quantum yield beyond the stokes limit by utilizing the commercialized AlGaAs laser diodes(LD) around 790 nm as pump sources [12-14]. Solid-state Tm lasers usually employ garnets (YAG, LuAG)[15-16], fluorides (YLF, LuLF)[17-18] or aluminate (YAP)[19] as host media. Among them, YAG is especially applicable for high power lasers because of its high thermal conductivity and excellent mechanical properties[20-21].

Approaches to realize high power Tm:YAG lasers via increasing the power of side- or end-pump LD with specially designed cavities have been intensively researched during the past few decades[22-26]. However, as the pump power increases there are increased energy losses due to heat generation and/or photon upconversion[27], especially when the doping concentration of Tm^{3+} is high[27], thereby a tradeoff exists between the laser power and efficiency. Much effort has been paid to resolve this contradiction by, such as, using low doping concentration of Tm^{3+}[28] and grad-doping technique[29], or by lowering the LD heat sink temperature[22]. As an alternative approach, we tried to solve the problem from the aspect of optical spectrum. Through strictly matching the LD spectrum with the optimal excitation peak of the Tm:YAG crystal, an output laser power over 10 W and meanwhile high slope efficiency (52.4%) and optical conversion efficiency (45.1%) were achieved[30]. The

pump LD is locked by volume Bragg gratings (VBGs), so that it has fixed wavelength centered at 784.9 nm and narrow bandwidth of 0.1 nm (full width at the half maximum, FWHM) independent on temperature and LD power. The stability of the LD assures the efficient pump of the crystal and evidently guarantees laser output with high quality and efficiency. However, it is still unknown whether the LD bandwidth is crucial for the achievement of high efficiency laser, which is of vital importance when selecting the pump laser source.

In this paper, composite Tm:YAG/YAG crystal was used as gain medium and a compact and high efficiency Tm:YAG/YAG laser was conducted by using the VBGs locked LD as pump source. The theoretical models were defined to give a detailed demonstration of spectral and thermal properties. Taking the quasi-three-level Tm:YAG laser as an example, we considered the spectral overlap between the pump spectrum and the measured absorption and excitation spectra to analyze the influence of pump spectral properties on the Tm laser efficiencies and thermal effects. The methods could be applied to other solid-state lasers and help to improve their laser efficiencies.

1 Theoretical model

1.1 Spectral model

Figure 1 shows the energy level scheme of Tm^{3+} ions along with the important electronic transitions associated with the laser radiation. Upon 780 nm LD pumping, Tm^{3+} ions are excited to the excited-state $^3H_4$, and relax nonradiatively to $^3H_5$ and then to $^3F_4$, a metastable state for the laser radiation. A cross-relaxation process, $^3H_4+{}^3H_6\rightarrow{}^3F_4+{}^3F_4$, also occurs, giving rise to two Tm^{3+} ions on $^3F_4$ by absorbing one pump photon. The quantum yield for $^3F_4$ luminescence can be calculated by[31]

$$\eta_{QY}=\frac{1+2\left(\frac{C_{Tm}}{C_0}\right)^2-\frac{\tau_0}{\tau_r}(1-\beta)}{1+\left(\frac{C_{Tm}}{C_0}\right)^2} \tag{1}$$

where C_{Tm} is the actual concentration of Tm^{3+}(3.5 at.%), C_0 denotes a critical concentration and equals to 0.5 at.%, τ_0 and τ_r are the lifetime and radiative lifetime of $^3F_4$ state (541 μs[31] and 1.4 ms[32]) respectively, and β is the branch ratio (0.16).

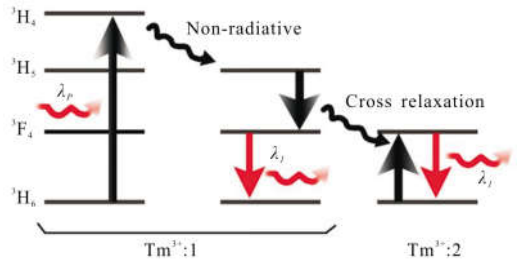

Fig.1 Energy level scheme of Tm^{3+} ions along with the important electronic transitions associated with the laser radiation. λ_P and λ_l represent the pump and laser wavelengths, respectively

The absorption coefficient α of a laser crystal is usually determined for a specific wavelength. Nevertheless, the commercialized LDs usually exhibit a considerable emission bandwidth; for example, 3 nm for 800 nm AlGaAs LD [33] and around 20 nm for 1.9 μm AlGaIn/AsSb LD [34]. In order to investigate the influence of LD bandwidth on the laser performance, an effective absorption coefficient α_{eff} is introduced[2-3]

$$\alpha_{eff}(\lambda_P,\Delta\lambda_P)=\frac{\int_{\Delta\lambda}A(\lambda)I_P(\lambda)\mathrm{d}\lambda}{\int_{\Delta\lambda}I_P(\lambda)\mathrm{d}\lambda} \tag{2}$$

where λ_P and $\Delta\lambda_P$ are the central wavelength and FWHM width of the LD, $A(\lambda)$ is the absorption spectrum of the crystal in unit of cm^{-1}, $I_P(\lambda)$ is the spectral profile of the LD, spanning a wavelength range of $\Delta\lambda$. The emission spectrum of the LD is measured by an optical spectrum analyzer (AQ6270C, YOKOGAWA) with a resolution of 0.02 nm. The absorption spectrum of YAG/Tm:YAG crystal is obtained by a PerkinElmer UV-VIS-NIR spectrometer (Lambda 950) with resolution of 0.1 nm.

Correspondingly, the effective excitation efficiency for a laser crystal, η_e, is calculated by[4]

$$\eta_e(\lambda_P,\Delta\lambda_P)=\frac{A_0\int_{\Delta\lambda}I_e(\lambda)I_P(\lambda)\mathrm{d}\lambda}{\int_{\Delta\lambda}I_P(\lambda)\mathrm{d}\lambda} \tag{3}$$

where A_0 is a coefficient factor, and $I_e(\lambda)$ is the spectral profile of the excitation spectrum of the crystal, which is measured by using a fluorescence spectrometer (FSP920C, Edinburgh Instruments) following the previous procedure[4].

1.2 Thermal model

Temperature distribution within the YAG/Tm: YAG crystal is determined by the heat transfer Poisson equation with given crystal boundary conditions. For a rectangular crystal, the equation is[16,35-36]:

$$K_x\frac{\partial^2T(x,y,z)}{\partial x^2}+K_y\frac{\partial^2T(x,y,z)}{\partial y^2}+K_z\frac{\partial^2T(x,y,z)}{\partial z^2}+q(x,y,z)=0 \tag{4}$$

where K_x, K_y, and K_z are the thermal conductivity coefficients along the x,y, and z axis respectively, and T is the temperature. The heat reflux, $q(x,y,z)$, can be written as

$$q(x,y,z)=\frac{\eta_h P_{\mathrm{in}}\alpha_{\mathrm{eff}}}{\pi\omega_P^2}\mathrm{e}^{-2(x^2+y^2)^2/\omega_P^4-\alpha_{\mathrm{eff}}(z-\mathrm{d}l)} \tag{5}$$

where P_{in} is the incident pump power, α_{eff} is the effective absorption coefficient, ω_P is the waist radius of the pump beam, dl is the length of undoped YAG crystal, and η_h is the quantum efficiency taking into account the quantum defect for Tm^{3+} luminescence ($\eta_h=1-\eta_{QY}\lambda_P/\lambda_l$, λ_P and λ_l are the pump and laser wavelength respectively).

Boundary conditions for a crystal with dimensions of $2a\times2b\times l$ meet the Dirichlet boundary condition at the four cooling facets and the Neumann condition at the other two facets exposed to air as follows:

$$\begin{aligned}
&-K_z\frac{\partial T(x,y,z)}{\partial z}|_{z=0}=h_{\mathrm{air}}(T_e-T(x,y,0))\\
&T(a,y,z)=T_0\\
&T(x,b,z)=T_0\\
&-K_z\frac{\partial T(\mathrm{x},y,z)}{\partial z}|_{z=l}=h_{\mathrm{air}}(T_e-T(\mathrm{x},y,l))\\
&T(-a,y,z)=T_0\\
&T(x,-b,z)=T_0
\end{aligned} \tag{6}$$

where T_e is the environmental temperature, h_{air} is the heat transfer coefficient of air, and T_0 is the heat sink temperature (15 ℃).

Neglecting high order terms, the optical path difference (OPD) for laser beam propagating along the z direction can be expressed as[37]

$$\mathrm{OPD}(r)=2\int_0^l\left[\frac{\partial n}{\partial T}+(n-1)(1+\nu)\alpha_T\right]\Delta T(r,z)\mathrm{d}z \tag{7}$$

where n is the refractive index of the crystal at 2 μm, ν is the Possion′s ration, α_T is the thermal expansion coefficient, ΔT (r,z) is the temperature difference between $T(r,z)$ and the heat sink temperature T_0, and r represents the distance away from the crystal resonator axis.

The thermal focus length, f_{th}, can be solved by the following equation:

$$\mathrm{OPD}(r)=\mathrm{OPD}_0-\frac{r^2}{f_{\mathrm{th}}} \tag{8}$$

where OPD_0 is the OPD at $r=\omega_P$.

2 Tm laser experiment

2.1 Experimental setup

A schematic diagram of the experimental laser setup is shown in Fig.2. The pump source is a 25 W fiber-coupled LD (core diameter: 400 μm, NA: 0.22), which is locked by VBGs so that both of its emission wavelength (784.9 nm) and bandwidth (0.1 nm) are insensitive to temperature ((20±5) ℃) and LD power. The focusing system contains two identical plano-convex lenses with coupling efficiency about 95%. The gain medium is a diffusion bounded crystal composed of a 3.5 at.% Tm:YAG crystal with dimensions of 3 mm×3 mm×6 mm and an undoped YAG crystal with dimensions of 3 mm×3 mm×2 mm. The gain medium is wrapped with indium foil and tightly mounted in a copper sink maintained for water cooling at 15 ℃. The pump waist is focused to be 200 μm in radius inside the crystal. The laser cavity has a length of 35 mm. The absorption efficiency of the pump beam is determined to be 88.47%. Dichroic mirror M1 is coated with high reflection (HR>99.7%) in the range of 1.88-2.15 μm and high transmission (AR>95%) at

750–850 nm, and the output coupler, M2, coated with high reflection (HR>99.7%) at the pump wavelength and partial transmission (3% or 5%) at the laser wavelength. DM is a dichroic beam-splitting mirror (45°, HR at the laser wavelength and AR at the pump wavelength). The calculated mode size of the laser in the composite Tm:YAG crystal is 145 μm.

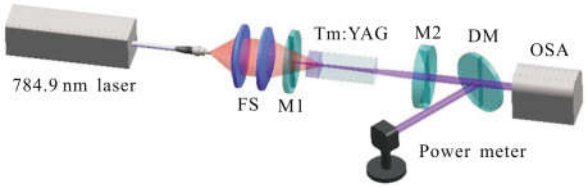

Fig.2 Schematic diagram of the experimental laser setup employed in the present study

2.2 Experimental results

Figure 3 (a) shows power properties of the Tm laser with output coupling of 3% and 5%, respectively. The solid lines are the linear fittings of the experimental data The inset shows the laser spectrum at the maximum output. A nearly identical laser threshold around 1.3 W was observed for the two output couplers. The slope efficiency and the optical conversion efficiency were determined to be 62.51% and 53.32% for the 3% output coupler, and 50.61% and 43.53% for the 5% output coupler, respectively. The relatively higher laser efficiencies as compared with Ref [4] are mainly attributed to reduced reabsorption losses, due to the shorter gain medium used in the study. As observed in Ref[38], the shorter of the Tm:YAG gain medium is, the higher of the laser efficiencies are. As a result, a maximum output power of 7.96 W at the absorbed LD power of 14.93 W was achieved. The laser efficiencies are among the highest ever reported in the literature, which may largely be attributed to the verified spectral method[38]. Within one hour monitoring, the stability of maximum output power is 7.96 W ±0.014 W. The relative root-mean-square fluctuation is 0.18%. The corresponding laser beam quality for the maximum output is shown in Fig.3(b), and the M^2 values were determined to be 1.13 and 1.22 along the horizontal and vertical directions, respectively. The inset shows the corresponding 2D and 3D beam profiles. With the increase of pump power, significant wavelength drift of the laser was observed (Fig.4), which is attributed to the reabsorption loss in stark levels of the Tm^{3+} ions [3]. The maximum laser wavelength drifted from 2 013.25 nm to 2 014.53 nm when increasing the laser power from 1.87 W to 14.93 W for the 3% output coupling, while for 5% output coupling the drift band was from 2 013.91 nm to 2014.26 nm. Etaloning effects originating from parallel planes of the gain medium and the cavity mirrors are probably responsible for the oscillating of separated longitudinal modes, especially because the cavity is of plano-plano type and the crystal is of standard cubic shape.

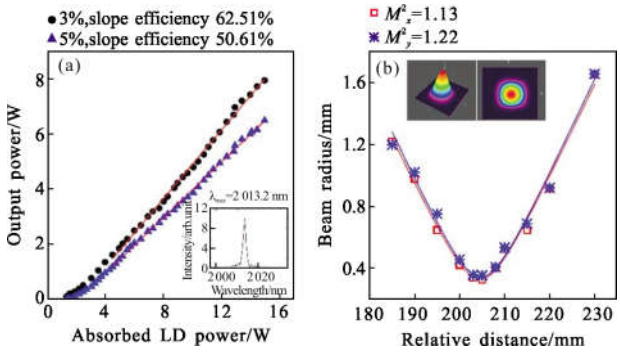

Fig.3 (a) Dependence of laser output power on the absorbed LD power for output couplers with 3% and 5% transmission respectively; (b) beam quality measured at the maximum output

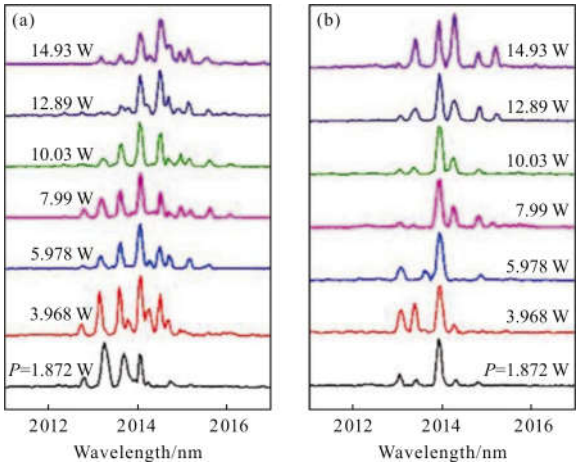

Fig.4 Wavelength drift of the Tm laser with increased absorbed pump power for output couplers of (a) 3%, and (b) 5%

3 Discussion

Figure 5 (a) shows the measured absorption and excitation spectra of the Tm:YAG crystal, from which an optimal pump wavelength around 785 nm can be determined by the overlap between the excitation and absorption peaks[4]. The LD pump spectrum with central wavelength of 784.9 nm and bandwidth of 0.1 nm matches well with the optimal pump peak. The LD spectrum is stretched through numerical interpolation to be with bandwidths of 1, 2, 3 nm (Fig.5 (b)), in order to reveal the influences of LD bandwidth and wavelength-drift on the spectral properties. The effective absorption coefficients for different LD bandwidths are then calculated according to Eq. (2) and shown in Fig.5(c), and the corresponding effective excitation efficiencies by Eq.(3) and shown in Fig.5 (d). As can be seen, when the pump wavelength with bandwidth around 0.1 nm locates within the maximum absorption and excitation peak of the crystal, larger effective absorption coefficient and excitation intensity can be obtained(maximum absorption coefficient of 2.89 cm^{-1} at 785.4 nm). If we set excitation intensity at this peak wavelength to be unity, the relative excitation efficiencies are 0.945 9, 0.889 8 and 0.854 4 when the LD bandwidths are broadened to be 1, 2, 3 nm, respectively. Commonly, AlGaAs LD has bandwidth near 3 nm and wavelength drift around 0.3 nm/℃. Considering the LD with central wavelength of 784.9 nm and working temperature change of ± 3 ℃, the LD wavelength would change from 784 nm to 785.8 nm with corresponding effective absorption coefficients changed from 2.25 cm^{-1} to 2.30 cm^{-1}, and the relative excitation efficiency changed from 0.801 3 to 0.846 7. However, when wavelengths of the LD with 0.1 nm bandwidth are fixed at 783.9 nm or 785.9 nm (accuracy limits of the designed 784.9 nm wavelength-locked LD), the absorption coefficients are 2.06 cm^{-1} and 2.72 cm^{-1} and corresponding the relative excitation efficiency are 0.695 9 and 0.734 1 respectively, which are comparable or lower than the value obtained using a normal 784.9 nm LD. Hence, if the LD wavelength locates significantly away from the optimal pump wavelength, LD with broad bandwidth is more attractive for a higher absorption and excitation efficiency, which is determined by the spectral profiles in Fig.5(a) and (b).

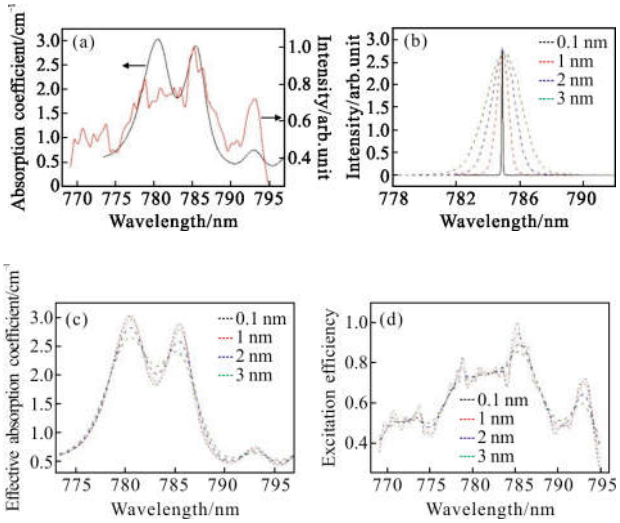

Fig.5 Experimentally measured (a) absorption (black line) and excitation (red line) spectra of the YAG/Tm:YAG crystal and (b) emission spectrum of the VBGs locked LD (solid line). The spectrum of the LD is broaden by mathematical method to those with FWHM bandwidths of 1, 2, 3 nm, respectively (dashed lines). Simulated spectra of (c) effective absorption coefficient and (d) excitation efficiency (relative to that of 0.1 nm bandwidth) for LD bandwidths of 0.1, 1, 2, 3 nm

In order to reveal the influence of pump bandwidth and wavelength drift on the thermal effects of the crystal, we further solved Eq. (4)−(8) by the finite difference method and using the parameters listed in Tab.1. At the maximum pump power around 14.93 W, Fig.6 shows the calculated temperature distributions within the YAG/Tm:YAG crystal for four LD bandwidths. The temperature distribution exhibits similar features for the four pump bandwidths, while the maximum temperature is slightly higher for the LD with bandwidths of 0.1 nm (52.49 ℃) than the

other ones (51.90, 50.43, 48.70 ℃ for bandwidths of 1, 2, 3 nm respectively), which is consistent with the evolution trend in effective absorption coefficients, as more heat is generated from higher absorption.

Tab.1 Parameters included in the thermal numerical simulations[39]

Parameters	Value
Poisson's ratio	0.3
Refractive index of Tm:YAG	1.81
Efficient absorption coefficient/cm^{-1}	2.7(FWHM=0.1 nm) 2.62(FWHM=1 nm) 2.52(FWHM=2 nm) 2.4(FWHM=3 nm)
Incident pump power/W	14.93
Temperature of cooling liquid/℃	15
Environment temperature/℃	22
Heat conductivity of YAG/W·(mm·K)$^{-1}$	1.4×10^{-2}
Heat transfer coefficient of air/W·(mm^2·K)$^{-1}$	0.5×10^{-6}
Pump beam waist/mm	0.2
Thermal expansion coefficient/℃$^{-1}$	7.8×10^{-6}
Thermal-optical coefficient/℃$^{-1}$	7.3×10^{-6}
Length of active part/mm	8
Length of un-doped part/mm	2

Thermal lens is an important factor to influence the laser stability and beam quality, especially under high power pumping. Based on the calculated effective absorption coefficient and temperature distribution, we further calculated the thermal focal length (TFL) using the OPD model for the four LD bandwidths with a wavelength-drift range from 780 nm to 785.5 nm (Fig.7). The dashed line points out the locked-wavelength of LD used in the present study. Figure 7 also shows the evolution of maximum temperature within the crystal with the pump bandwidth. Interestingly, the TFLs remain nearly unchanged when varying the LD bandwidth within a wavelength-drift range from 780 nm to 785.4 nm. For LD with central wavelength of 784.9 nm and bandwidths of 0.1, 1, 2, 3 nm, the TFLs are 43.71, 43.79, 43.88, 44.02 mm respectively, where the fluctuation in TFLs is 0.7%, an order of magnitude lower than that in the maximum temperatures. The independence of TFL on the pump bandwidth and wavelength drift around the 785 nm pump band is determined by the absorption profile of Tm:YAG crystal which could be different in other rare-earth doped gain media.

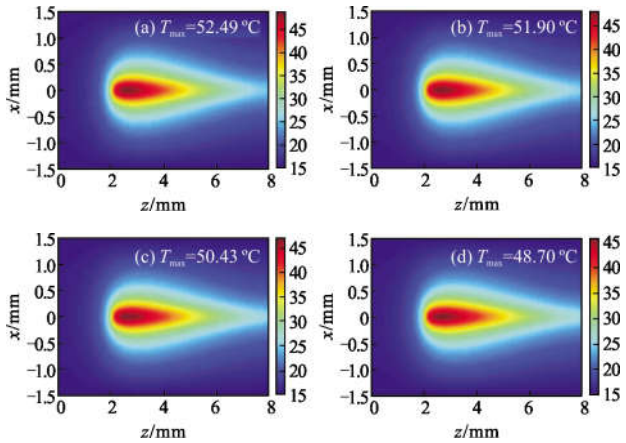

Fig.6 Simulated temperature distributions within the YAG/Tm:YAG crystal at the maximum pump power around 14.93 W when using different LD bandwidths of (a) 0.1 nm, (b) 1 nm, (c) 2 nm, and (d) 3 nm. The maximum temperatures for the four LD bandwidths are 52.49, 51.90, 50.43, 48.70 ℃ respectively

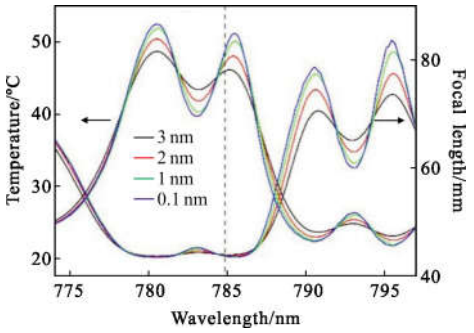

Fig.7 Evolution of the maximum temperature and TFL within the YAG/Tm:YAG crystal influenced by the LD bandwidth and wavelength-drift

4 Conclusion

We have analyzed the influences of LD bandwidth and wavelength drift on spectral efficiencies and thermal effects of solid lasers by taking a narrowband LD pumped Tm laser as an example. In the laser experiment, a maximum output power of

7.96 W with slope efficiency of 62.51% was obtained, where the laser wavelength-drift around 2 014 nm originated from reabsorption loss was characterized. The M^2 values are 1.13 and 1.22 along the horizontal and vertical directions. Wavelength-drift were also measured from 2 013.91 nm at 1.87 W to 2 014.26 nm at 14.93 W, when using 5% output coupling. When using 3% output coupling, the wavelength-drift ranged from 2 013.25 nm at 1.87 W to 2 014.53 nm at 14.93 W. The effective absorption coefficients and corresponding relative excitation efficiency for different LD bandwidths were obtained. When the LD wavelength with bandwidth of 0.1 nm located within the maximum absorption and excitation peak of the crystal, larger effective absorption coefficient and excitation intensity were achieved. When the LD has a central wavelength of 784.9 nm and ±3 ℃ temperature change, the LD wavelength could drift from 784 nm to 785.8 nm. The corresponding effective absorption coefficients would range from 2.25 cm^{-1} to 2.30 cm^{-1}. The relative excitation efficiency changed from 0.801 3 to 0.846 7. According to the theoretical analysis, when the wavelength was locked at the optimal pump peak, narrow-bandwidth pump sources stabilized by etalon or VBGs make significant improvement in absorption and excitation efficiencies and hence the lasing efficiencies. When significant pump wavelength-drift exists, broad pump bandwidth would be more attractive for a smooth efficient absorption and relative excitation spectral profiles. In the Tm:YAG laser, although maximum temperature in gain medium will be slight influenced by pump bandwidth and wavelength-drift, the TFL is insensitive with them, which is determined by the absorption spectrum of the gain medium. The models here produce an effective way for determining the pump source by considering the pump bandwidth and wavelength-drift.

References:

[1] Ji E, Liu Q, Cao X, et al. Resonantly fiber-coupled diode-pumped Ho^{3+}: $YLiF_4$ laser in continuous-wave and Q-switched operation [J]. ***IEEE Journal of Quantum Electronics***, 2016, 52(7): 1-8.

[2] Lamrini S, Koopmann P, Schäfer M, et al. Efficient high-power Ho: YAG laser directly in-band pumped by a GaSb-based laser diode stack at 1.9 μm [J]. ***Applied Physics B***, 2012, 106(2): 315-319.

[3] Huang H, Huang J, Liu H, et al. Manipulating the wavelength-drift of a Tm laser for resonance enhancement in an intra-cavity pumped Ho laser [J]. ***Optics Express***, 2018, 26(5): 5758-5768.

[4] Huang H, Huang J, Liu H, et al. High-efficiency Tm-doped yttrium aluminum garnet laser pumped with a wavelength-locked laser diode [J]. ***Laser Physics Letters***, 2016, 13(9): 095001.

[5] Fan T Y, Huber G, Byer R L, et al. Continuous-wave operation at 2.1 μm of a diode-laser-pumped, Tm-sensitized Ho: $Y_3Al_5O_{12}$ laser at 300 K [J]. ***Optics Letters***, 1987, 12(9): 678-680.

[6] Gao C, Gao M, Zhang Y, et al. Stable single-frequency output at 2.01 μm from a diode-pumped monolithic double diffusion-bonded Tm: YAG nonplanar ring oscillator at room temperature[J]. ***Optics Letters***, 2009, 34(19): 3029-3031.

[7] Fan T Y, Huber G, Byer R L, et al. Spectroscopy and diode laser-pumped operation of Tm, Ho: YAG[J]. ***IEEE Journal of Quantum Electronics***, 1988, 24(6): 924-933.

[8] Scholle K, Lamrini S, Koopmann P, et al. 2 μm laser sources and their possible applications[C]//Frontiers in Guided Wave Optics and Optoelectronics. InTech, 2010: 10.5772/39538.

[9] Koch G J, Dharamsi A N, Fitzgerald C M, et al. Frequency stabilization of a Ho: Tm: YLF laser to absorption lines of carbon dioxide[J]. ***Applied Optics***, 2000, 39(21): 3664-3669.

[10] Theisen D, Ott V, Bernd H W, et al. CW high power IR-laser at 2 μm for minimally invasive surgery[C]//European Conference on Biomedical Optics. Optical Society of America, 2003: 5142_96.

[11] Liu J, Shen D, Huang H, et al. Highly efficient Tm-doped yttrium aluminum garnet ceramic laser based on the novel fiber-bulk hybrid configuration[J]. ***Applied Physics Express***, 2013, 6(9): 092107.

[12] Elder I F, Payne M J P. Lasing in diode-pumped Tm: YAP, Tm, Ho: YAP and Tm, Ho: YLF[J]. ***Optics Communications***, 1998, 145(1-6): 329-339.

[13] Sato A, Asai K, Itabe T. Double-pass-pumped Tm: YAG laser with a simple cavity configuration [J]. ***Applied Optics***,

1998, 37(27): 6395-6400.

[14] Rustad G, Stenersen K. Modeling of laser-pumped Tm and Ho lasers accounting for upconversion and ground-state depletion [J]. ***IEEE Journal of Quantum Electronics***, 1996, 32(9): 1645-1656.

[15] Zhu H, Zhang Y, Zhang J, et al. 1.96 μm Tm:YAG ceramic laser[J]. ***IEEE Photonics Journal***, 2017, 9(6): 1506607.

[16] Wu C, Ju Y, Li Y, et al. Diode-pumped Tm: LuAG laser at room temperature [J]. ***Chinese Optics Letters***, 2008, 6(6): 415-416.

[17] Yu H, Petrov V, Griebner U, et al. Compact passively Q-switched diode-pumped Tm: $LiLuF_4$ laser with 1.26 mJ output energy[J]. ***Optics Letters***, 2012, 37(13): 2544-2546.

[18] Soulard R, Tyazhev A, Doualan J L, et al. 2.3 μm Tm^{3+}: YLF mode-locked laser [J]. ***Optics Letters***, 2017, 42(18): 3534-3536.

[19] Zhang Haikun, Huang Jiyang, Zhou Cheng, et al. CW mode-locked Tm:YAP laser with semiconductor saturable-absorber at around 2 μm [J]. ***Infrared and Laser Engineering***, 2018, 47(5): 0505003. (in Chinese)

[20] Yumoto M, Saito N, Urata Y, et al. 128 mJ/Pulse, laser-diode-pumped, Q-switched Tm: YAG laser [J]. ***IEEE Journal of Selected Topics in Quantum Electronics***, 2015, 21(1): 364-368.

[21] Zhan M J, Zou Y W, Lin Q F, et al. Ti:sapphire pumped passively mode-locked Tm:YAG ceramic laser [J]. ***Acta Physica Sinica***, 2014, 63(1): 014205. (in Chinese)

[22] Cao D, Peng Q, Du S, et al. A 200 W diode-side-pumped CW 2 μm Tm: YAG laser with water cooling at 8 ℃[J]. ***Applied Physics B***, 2011, 103(1): 83-88.

[23] Beach R J, Sutton S B, Skidmore J A, et al. High-power 2-μm wing-pumped Tm:YAG laser [C]//Conference on Lasers and Electro-Optics, 1996: 319.

[24] Honea E C, Beach R J, Sutton S B, et al. 115-W Tm: YAG diode pumped solid state laser [J]. ***IEEE Journal of Quantum Electronics***, 1997, 33(9): 1592-1600.

[25] Zhang X F, Xu Y T, Li C M, et al. A continuous-wave diode-side-pumped Tm:YAG laser with ouput 51 W [J]. ***Chinese Physics Letters***, 2008, 25(10): 3673-3675.

[26] Wang C, Niu Y, Du S, et al. High power diode side pumped rod Tm: YAG laser at 2.07 μm[J]. ***Applied Optics***, 2013, 52(31): 7494-7497.

[27] Eichhorn M. Quasi three level solid state lasers in the near and mid infrared based on trivalent rare earth ions [J]. ***Applied Physics B***, 2008, 93(2-3): 269.

[28] Eichhom M, Kieleck C, Hirth A. OP-GaAs OPO pumped by a Q-switched Tm, Ho:Silica fiber laser [C]//Conference on Lasers and Electro-Optics/International Quantum Electronics Conference, 2009: CWH2.

[29] Cheng X, Shang J, Jiang B. Analysis of the thermal effects in diode-pumped Tm: YAG ceramic slab lasers [J]. ***Laser Physics***, 2017, 27(3): 035803.

[30] Huang H Z, Huang J H, Liu H G, et al. High-efficiency Tm-doped yttrium aluminum garnet laser pumped with a wavelength-locked laser diode [J]. ***Laser Physics Letters***, 2016, 13(9): 095001.

[31] Honea E C, Beach R J, Sutton S B, et al. 115-W Tm: YAG diode-pumped solid-state laser [J]. ***IEEE Journal of Quantum Electronics***, 1997, 33(9): 1592-1600.

[32] Caird J, Deshazer L, Nella J. Characteristics of room-temperature 2.3-μm laser emission from Tm^{3+} in YAG and $YAlO_3$[J]. ***IEEE Journal of Quantum Electronics***, 1975, 11(11): 874-881.

[33] Li B, Ding X, Sun B, et al. 12.45 W wavelength-locked 878.6 nm laser diode in-band pumped multisegmented Nd: YVO_4 laser operating at 1342 nm [J]. ***Applied Optics***, 2014, 53(29): 6778-6781.

[34] Scholle K, Fuhrberg P. In-band pumping of high-power Ho: YAG lasers by laser diodes at 1.9 μm [C]//Conference on Lasers and Electro-optics. Optical Society of America, 2008: CTuAA1.

[35] Zhang Haiwei, Sheng Quan, Shi Wei, et al. Thermal distribution characteristic of high-power laser double-cladding thulium-doped fiber amplifier [J]. ***Infrared and Laser Engineering***, 2017, 46(6): 0622004.

[36] Cheng X, Shang J, Jiang B. Analysis of the thermal effects in diode-pumped Tm: YAG ceramic slab lasers [J]. ***Laser Physics***, 2017, 27(3): 035803.

[37] Pfistner C, Weber R, Weber H P, et al. Thermal beam distortions in end-pumped Nd: YAG, Nd: GSGG, and Nd: YLF rods[J]. ***IEEE Journal of Quantum Electronics***, 1994, 30(7): 1605-1615.

[38] Huang H, Gao P, Liu H G, et al. Validation of spectrum method for improving efficiency of continuous-wave & Q-switched Tm-doped yttrium aluminum garnet laser [J]. ***Science China Physics, Mechanics & Astronomy***, 2018, 61(3): 034221.

[39] Chen X, Wu J, Wu C, et al. Analysis of thermal effects in a pulsed laser diode end pumped single-ended composite Tm: YAG laser[J]. ***Laser Physics***, 2015, 25(4): 045003.